



ARTICLE

Fabrication of Baking-Free Bricks Using Gold Tailings and Cemented Materials with Low Alkalinity

Jiamao Li^{1,2,*}, Tao Si¹, Lin Li¹, Chuangang Fan^{1,*}, Zhaofang He³ and Yuandi Qian³

¹School of Materials Science and Engineering, Anhui University of Technology, Maanshan, 243032, China

²Key Laboratory of Green Fabrication and Surface Technology of Advanced Metal Materials, Ministry of Education, Maanshan, 243002, China

³China MCC17 Group Co., Ltd., Maanshan, 243000, China

*Corresponding Authors: Jiamao Li. Email: agdjiaaolee@126.com; Chuangang Fan. Email: chgfan67@163.com

Received: 01 November 2021 Accepted: 23 December 2021

ABSTRACT

The purpose of this paper was using gold mine tailings and cemented materials with low alkalinity to fabricate baking-free bricks. The obtained baking-free brick samples were evaluated by unconfined compressive strength (UCS), water absorption percentage, freezing-thawing cycle, and drying-wetting cycle. The microstructures of the baking-free brick samples were analyzed using X-ray diffraction (XRD) and scanning electron microscope (SEM) techniques. The baking-free brick specimens cured for 28 days with the addition of 10% mixing water consumption and 1:6 cement/tailing ratio tended to obtain favorable comprehensive properties such as a high compressive strength of 15.15 MPa, a low water absorption percentage of 11.8%, excellent freezing-thawing resistance with a 8.9% UCS loss rate after 15 freezing-thawing cycles and good drying-wetting resistance with a 11% UCS loss rate after 10 drying-wetting cycles. The XRD and SEM test results verified that different kinds of hydrate products including C-S-H and C-S-A-H gels, and ettringite were produced during hydration process, which were responsible for good physical, mechanical properties, and durability of the obtained baking-free bricks. Therefore, the experimental results showed that it was practical and reasonable to utilize the homemade cementitious materials in our laboratory to stabilize the gold tailings for production of baking-free bricks, which still met the requirements of major regional construction standards in some countries.

KEYWORDS

Baking-free brick; low alkali cementitious binder; solid waste utilization; compressive strength; freezing-thawing; drying-wetting

1 Introduction

Gold has long been considered a symbol of wealth due to its scarcity and performance stability. According to incomplete statistics, the mined gold from gold ores has been up to 190,000 tons since 1950 [1]. Nowadays, gold is not only an asset but also a commodity, which is very active in the field of economic circulation and international financial market. Moreover, the industrial demand for gold has increased sharply with the rapid growth of electronic products such as smart-phones and computers [2,3]. Fewer and fewer high-quality gold mine ores have kept up the price of gold. Clearly, in gold mineral



processing, low-quality gold mine ores will produce more gold mine tailings inevitably. For example, each year in China, at least 24.5 million tons of gold mine tailings are generated since 1 ton of gold raw ore can produce 0.95 ton gold mine tailings [4]. These huge amounts of gold mine tailings are very hard to be handled with and have to be disposed of in surface impoundments, which cause danger for the environment, social assets, and human health due to their including potentially toxic elements. Therefore, the heavy application of gold mine tailings is crucially required.

In recent years, a variety of researches have been performed on developing effective techniques to utilize these tailings widely including the recovery of associated valuable elements, the production of construction materials, glass fibers, and ceramics [1,5–10]. Guo et al. [5] recovered gold and silver elements with high recovery efficiencies of 99.92% and 87.78% from a refractory gold tailing by an iodination roasting technology. They concluded that this new technology was a promising route to recover different kinds of gold and silver residues from metal tailings. Using the gold mine tailings as main siliceous materials, Yang et al. [6] successfully prepared autoclaved aerated concrete to realize the resource utilization of gold mine tailings and found that the compressive strength of the as-prepared concrete can meet the needs of A3.5, B06 level of the autoclaved aerated concrete completely, which is regulated by the Chinese standard GB/T 11969-2008. In order to develop a cost-effective technology and low the environmental hazards, Gitari et al. [7] investigated the physicochemical and mineralogical performances of gold mine tailings and found that the gold mine tailings required blending with Al_2O_3 -rich materials to obtain the optimized mechanical strength for the fabrication of geopolymeric construction materials. They also found that the gold mine tailings with similar particle size to fine sand possessed potential application in the conventional brick manufacture as aggregates. More recently, according to this idea, Wei et al. [1] found that gold mine tailings were prospective siliceous materials for the production of sintered bricks. However, the sintering process of conventional clay bricks results in a lot of energy consumption and CO_2 emissions [11]. Furthermore, in China, nowadays many cities have made some strict laws and regulations to forbid producing and using of conventional clay bricks. Numerous studies have shown that utilizing waste materials to replace clay for the production of baking-free bricks is feasible [12–25]. These results have indicated that this technology may be a potential application in the field of waste treatment for producing low-cost unfired green bricks. In addition, according to the above literature researches, this replacement clay with waste materials only needs a small quantity of binder for the production of baking-free bricks. From a recycling point of view, this strategy seems to be more meaningful. However, the related investigations on the production of baking-free bricks using gold mine tailings and cemented materials with low alkalinity are relatively insufficient so far.

In the present work, the factors influencing the performances of the baking-free bricks that were fabricated by the raw materials of gold mine tailings together with low alkalinity binders were investigated in detail. The effects of mixing water consumption, cement/tailing ratio, freezing-thawing cycle, and drying-wetting cycle on the performances of the baking-free bricks were studied using single-factor experiments. The current results will give a potential route for solving the safety and environmental pollution problems caused by the massive accumulation of gold mine tailings.

2 Materials and Methods

2.1 Raw Materials

2.1.1 Gold Mine Tailing

The gold mine tailing used in this work was provided by Zhaoyuan Mining Co., Ltd., located in Shandong Province of China. The chemical compositions of the main raw materials used in the current work were identified by an X-ray Fluorescence Spectrometer (XRF, ARL ADVANT'X Intellipower™ 3600, Thermo Fisher Scientific, USA). The results are displayed in Table 1. It can be seen that SiO_2 is the main component of the gold mine tailing, accounting for 70.14 wt%, followed by Al_2O_3 (17.30 wt%)

and M_2O (8.73 wt%). Clearly, the gold mine tailing is rich in SiO_2 , short of CaO compared with slag powder and 42.5 ordinary Portland cement in view of chemical composition.

Table 1: Chemical compositions of the main raw materials (wt%)

Raw materials	SiO_2	Al_2O_3	K_2O	Na_2O	CaO	Fe_2O_3	MgO	TiO_2	SO_3
Gold mine tailings	70.14	17.30	4.95	3.78	1.87	0.72	0.54	–	–
Slag powder	32.90	17.10	–	0.85	37.60	0.56	7.90	1.40	0.75
Fly ash	56.17	29.01	2.26	0.32	5.42	3.72	1.29	0.77	0.80
42.5 ordinary Portland cement	22.00	9.60	–	–	59.80	3.00	1.60	0.45	2.10

The particle size distribution of the gold mine tailing was measured by a particle size analyzer (Rise-2006, Jinan Runzhi Technology Co., Ltd., China) and the result is shown in Fig. 1. According to the tailings classification [26], the gold mine tailing used in this study can be categorized as a fine tailing (the proportion of $<20 \mu m$ is larger than 60%). Moreover, the gold mine tailing is free of sulphide minerals.

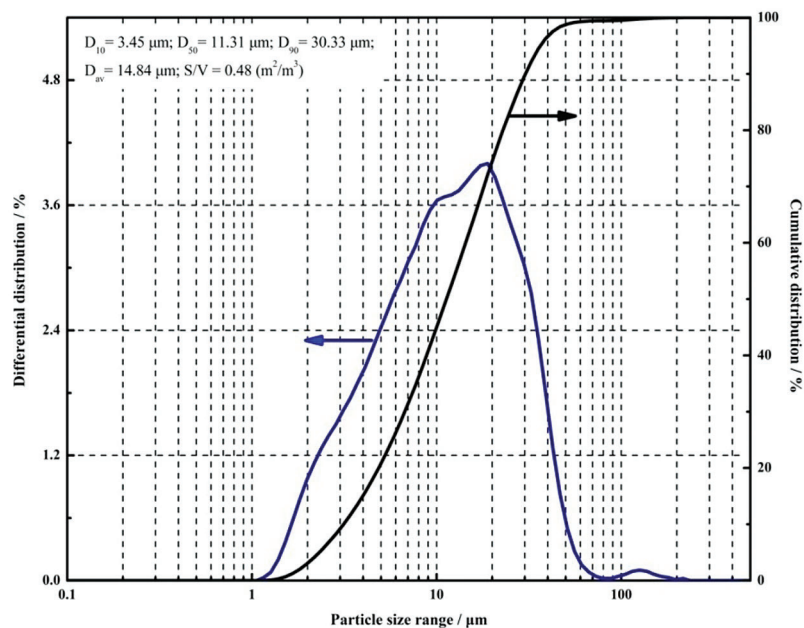


Figure 1: Particle size distribution of the gold mine tailing

2.1.2 Cemented Materials with Low Alkalinity

The cemented materials were synthesized by our lab using slag powder, fly ash, 42.5 ordinary Portland cement, Na_2SO_4 , CaO , and $CaSO_4$ according to a designed proportion. The pH value of the leaching solution of the as-prepared cemented materials was about 9.8, which was measured using a digital display pH-meter (PHS-25, Shanghai INESA Scientific Instrument Co., Ltd., China).

Grade-S95 slag powder with a density of 2.90 g/cm^3 and a specific surface area of $410 \text{ m}^2/\text{kg}$ was taken from Anhui Magang Jiahua New Building Materials Co., Ltd. of China. Its quality coefficient K was calculated as follows:

$$K = \frac{w(\text{CaO} + \text{MgO} + \text{Al}_2\text{O}_3)}{w(\text{SiO}_2 + \text{MnO}_2 + \text{TiO}_2)} \quad (1)$$

The calculated K value of the slag powder was 1.808 (its chemical composition is shown in Table 1), which is larger than 1.2. According to the provisions of the Chinese standard GB/T 203-2008, $K \geq 1.2$ is needed. Generally, the larger the K value, the higher the potential activity of the slag powder. Therefore, the slag powder used in this study has high potential activity.

Grade-I fly ash with a density of 2.29 g/cm^3 and a specific surface area of $242 \text{ m}^2/\text{kg}$ was purchased from the Maanshan No. 2 power plant of China. Its activity index H_{28} was measured based on the Eq. (2):

$$H_{28} = \frac{R}{R_0} \times 100\% \quad (2)$$

where R and R_0 were the 28 days compressive strength of test mortar and contrast mortar, respectively. The measured activity index of the fly ash used in this study was 76% (its chemical composition is listed in Table 1).

In the experiment, 42.5 ordinary Portland cement with a specific surface area of $360 \text{ m}^2/\text{kg}$ was provided by Anhui Conch Cement Co., Ltd. of China, its chemical composition is shown in Table 1. Na_2SO_4 , CaO , and CaSO_4 were analytical grade and all of them were provided by Sinopharm Chemical Reagent Co., Ltd. of China. They were directly used in the experiment without any further purification.

2.2 Preparation of Baking-Free Bricks

Table 2 shows the mix proportion design of the baking-free bricks fabricated by the gold mine tailings and the cementitious materials with low alkalinity. According to the design, a total of two series (each series includes four groups of the samples) were fabricated. The cement/tailings ratio was denoted as the mass ratio of the cementitious materials to the gold mine tailings. As indicated in Table 2, the series BW and BC were used to study the influences of the mixing water consumption and the cement/tailings ratio on the performances of the baking-free bricks, respectively. In addition, some samples of the BC series after 28 days of curing time were conducted on freezing-thawing cycle and drying-wetting cycle tests.

Table 2: Mix proportion design of the baking-free bricks

Series	Mixing water consumption (%)	Cement/tailings ratio	Curing age (days)
BW	6	1:6	28
	8		
	10		
	12		
BC	10	1:4	3, 7, 28
		1:6	3, 7, 28
		1:8	3, 7, 28
		1:10	3, 7, 28

Initially, a certain amount of slag powder, fly ash, 42.5 ordinary Portland cement, Na_2SO_4 , CaO , and CaSO_4 were weighed using an electronic balance accurately, respectively. Then these powders were mechanical mixed and ball-milled in a horizontal ball mill for about 60 min using steel balls with different diameters as milling media to obtain the cementitious binders with low alkalinity. It is necessary for the gold mine tailings to perform a pretreatment since the fresh tailings generally contain 20–40 wt%

moisture. In this study, the tailings were stored for about 48 h, performing a centrifugal solid-liquid separation. Then, they were dried in a drying oven and were ground by a 100-mesh sieve. Subsequently, the sieved tailings and the cementitious binders were weighed according to various cement/tailings ratios and were mixed homogeneously in a manual mixer. The desired water was added slowly to the mixture for obtaining a uniform paste. The paste was poured into a cylindrical mould with a diameter of 30 mm and a height of 30 mm, and was compacted under a pressure of 20 MPa for 5 min. After being removed from the die, the compacted samples were sealed with plastic wrap and were cured at $25 \pm 3^\circ\text{C}$ and relative humidity of $90 \pm 5\%$ in a curing box. After reaching a desired curing age, a series of performance tests on the baking-free bricks were conducted.

2.3 Test Methods

2.3.1 Unconfined Compressive Strength

Based on the Chinese standard GB/T 4111-2013, the unconfined compressive strength (UCS) of the baking-free brick was performed using an electronic universal testing machine (WDW-30, Jinan Metus Testing Technology Co., Ltd., China) with the maximum capacity of 30 kN. The peak failure load P was shown in the machine to determine the unconfined compressive strength according to Eq. (3).

$$\sigma = \frac{P}{A} \quad (3)$$

where σ , P and A are the UCS, the failure load, and the compression area of the sample facing the loading direction, respectively. The typical baking-free sample and the specific UCS test process are shown in Fig. 2. The baking-free brick sample was loaded at a constant rate of 1 kN/s until it was broken. Meanwhile, a compression loading rate of 1 mm/min was adopted. It is noted that the UCS value was obtained by the average of the UCS values of the three samples with the same preparation parameter.

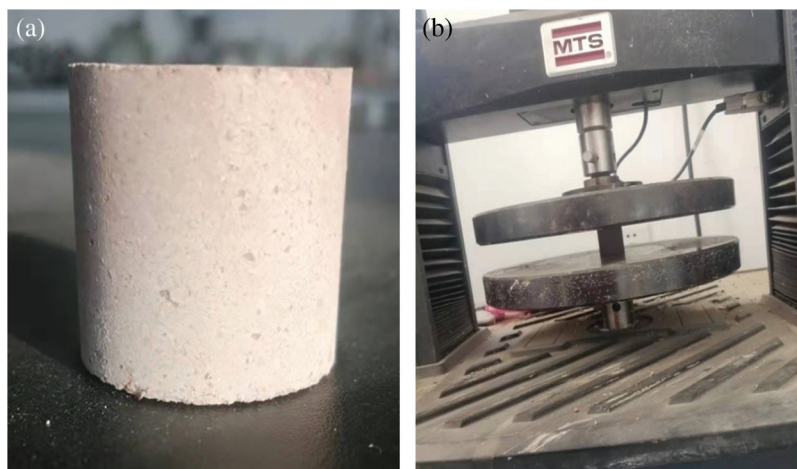


Figure 2: Typical baking-free sample (a) and specific UCS test process (b)

2.3.2 Water Absorption Test

The water absorption capacity can be characterized by the 24 h water absorption rate of baking-free bricks (see Fig. 3) that could be measured according to the Archimedes method. The test samples were dried absolutely at 105°C until obtained a constant weight m_0 . Subsequently, they were immersed in water at $20 \pm 2^\circ\text{C}$ for 24 h and then taken out to measure for obtaining another weight m_1 by wiping the surface water using a wet towel. The water absorption rate W_m was calculated based on Eq. (4).

$$W_m = \frac{m_1 - m_0}{m_0} \times 100\% \quad (4)$$



Figure 3: Baking-free samples in a water tank during the water absorption test

2.3.3 Drying-Wetting Cycle Test

Following the 28 days curing age, the baking-free brick samples suffered the drying-wetting cycle. In this work, the drying-wetting cycles were 0, 3, 5, 7, and 10, respectively. One drying-wetting cycle was defined as that a baking-free brick sample was wetted for 48 h via immersing it in tap water at room temperature (20°C) and then it was dried to its initial dry weight, then wetted again to swell. Finally, the UCS of these samples was measured using an electronic universal testing machine. The typical baking-free sample after 10 drying-wetting cycles test is displayed in [Fig. 4a](#).

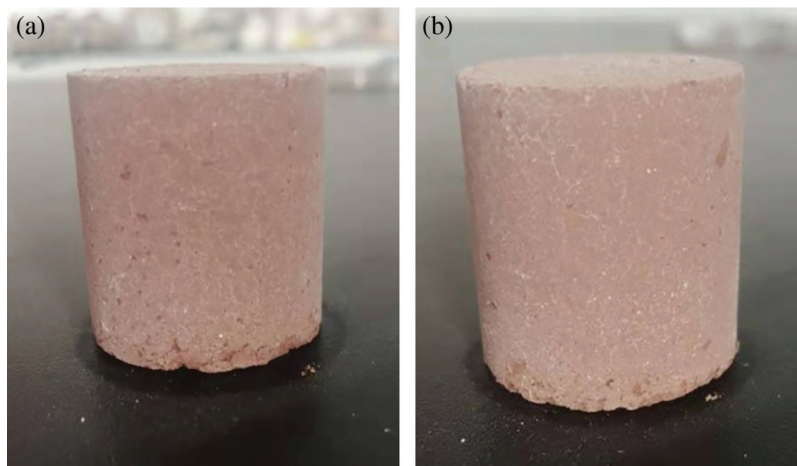


Figure 4: Typical baking-free samples after 10 drying-wetting cycles test (a) and 20 freezing-thawing cycles test (b)

2.3.4 Freezing-Thawing Cycle Test

After curing for 28 days, the baking-free brick samples were subjected to the freezing-thawing cycle test. In this work, the freezing-thawing cycles were 0, 3, 7, 15, and 20, respectively. A freezing-thawing cycle was composed of thawing the samples in water at 20°C for 4 h followed by freezing them at -15°C for 4 h in a low-temperature freezer. Subsequently, the UCS of the samples was measured and then the UCS loss was obtained by comparing with the value before the freezing-thawing cycle. In the case of dry freezing, wrapped a fresh-keeping film on the surface of the baking-free brick sample to prevent the loss of water, and then placed it in the low-temperature test chamber. In the case of wet freezing, soaked the baking-free brick sample in water for 1 day, took it out, wiped the surface water with a dry cloth, put on a fresh-keeping film, and placed it in a low-temperature freezer for the freezing-thawing cycle test. The typical baking-free sample after 20 freezing-thawing cycles test is presented in Fig. 4b.

2.3.5 Leaching Test

To explore the potential environmental effect of the baking-free bricks, the concentration of leached heavy metals in the leachate of the baking-free bricks was determined by an ICP emission spectrometer ICPS-7510 PLUS of Japan according to the Chinese standards GB 5085.3-2007. By mixing 100 water with 10 g powder of crushed brick specimens at 28 days curing age, a turbid liquid was prepared. Subsequently, the turbid liquid was magnetically stirred at a speed of 200 r/min for 2 h. Finally, the leachate was obtained by filtering the turbid liquid.

2.3.6 XRD and SEM Analysis

Phase structure of the sample after 28 days of moist curing was performed using a diffractometer system XRD D8 Advance of Germany with Cu K α radiation. The sample was ground to a fine powder (passing through 100 mesh square hole sieve) and then the XRD analyses were conducted with a 2 θ range of 20–80°C with a scanning speed of 4 °C/min. Before XRD identification, the samples that have been subjected to UCS test were stored into ethanol for 3 days to terminate the hydration process and were dried for about 8 h to obtain the constant weight. Microstructure observation was carried out by a SEM machine JSM6490 of Japan with a working voltage of 20 kV. Before observation, the fragments of the crushed samples were coated with a layer of gold.

3 Results and Discussion

3.1 Effect of Mixing Water Consumption on the UCS of the Baking-Free Brick Specimens

Mixing water consumption is one of the significant factors to influence the performances of baking-free bricks. Therefore, we investigated its effect on the UCS of the baking-free bricks using single-factor experiment, as shown in Table 2. Fig. 5 illustrates the relationship between the mixing water consumption and the UCS after 28 days of curing age. As displayed in Fig. 5, the 28 day UCS of the baking-free bricks increases from 13.17 MPa to 15.15 MPa as the mixing water consumption increases from 6% to 10%. The reason is that the increase of the mixing water consumption improves the inter-adhesion between particles in the sample and then makes the structure of the sample tight. As the mixing water consumption is 12%, the UCS sharply decreases from 15.15 MPa to 12.22 MPa. Excessive water evaporation will lead to more pores in the brick sample and even deformation of the brick sample, which ultimately results in a reduction in the UCS.

Since the raw materials and technical parameters in the manufacture of baking-free bricks differ from each other, the existing researches cannot give any specific advices on appropriate mixing water consumption. Zhang et al. [27] found that the compressive strength increased with an increase in molding water content up to 26%, whereas decreased at higher water content when the molding water content varies from 20% to 29%. The research results of Wattanasiriwech et al. [15] indicated that a continuous increase in the compressive strength was found in the investigated range of 15%–20%. They thought that

the diminishing of pore size with the increase of molding water content was responsible for the increase in the compressive strength of cement stabilized mud bricks. Zhao et al. [28] reported that when the water content varied in a range of 6%–8.5%, the fabricated bricks could obtain the optimum compressive strength. However, in another study [29], a continuous reduction in the compressive strength was observed for the production of red bricks using red mud and fly ash as raw materials and mud and fly ash activated using $\text{Ca}(\text{OH})_2$ and Na_2CO_3 as activators when the water content in mixture increases. An explicit mechanism of action for mixing water consumption remains to be further study.

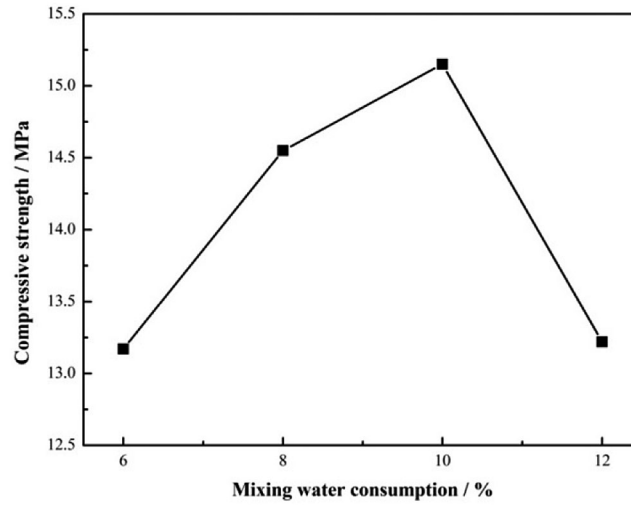


Figure 5: Effect of mixing water consumption on the unconfined compressive strength of the baking-free bricks

3.2 Effect of Cement/Tailings Ratio on the UCS and Water Absorption Capacity of the Baking-Free Brick Specimens

Fig. 6 shows the effect of cement/tailings ratio on the UCS development of the baking-free bricks after 3 days, 7 days, and 28 days of curing age. As shown in Fig. 6, the UCS decreases with the decrease of the cement/tailing ratio. Namely, when the content of the binder in the baking-free brick sample increases, the UCS increases. However, the effect of the cement/tailings ratio on the strength development of the brick sample with various curing ages is different. At the 3 days curing age, no significant change in the strength is found, only varying from 7.28 MPa to 8.47 MPa. Moreover, these strength values are lower than the mold pressure (10.00 MPa) of the brick samples. In our current work, the UCS at the 28 days curing age was taken as the final strength. It is clearly seen in Table 3 that the 3 days UCS development rate is remarkably low than the 7 days UCS development rate. Compared with the cement/tailing ratio, the curing age has a more significant effect on the early strength of the baking-free bricks. The reason is that too short a curing age cannot produce enough hydration products such as C-S-H and C-A-S-H to fill void spaces inside the bricks and then improve the UCS due to the secondary hydration characteristics of the mixed binders with low alkalinity. With the decrease of cement/tailings ratio from 1:4 to 1:10, the UCS of the brick specimens at 7 days and 28 days curing age decreases sharply from 14.00 MPa to 10.04 MPa and from 18.00 MPa to 13.48 MPa, respectively. The enhanced strength for those with high cement/tailings ratio should be attributed to the role of the cementitious binders. The slag powder, cement and fly ash can fill the spaces between the grains of gold mine tailings and therefore make the sample obtain a better size distribution, leading to a lower porosity. In addition, the slag powder and fly ash in the mixed binders have enough time to react with $\text{Ca}(\text{OH})_2$ generated from the cement hydration and

hence produce more C-S-H and C-A-S-H. These hydration products will occupy more void spaces inside the brick samples and form more compact structures.

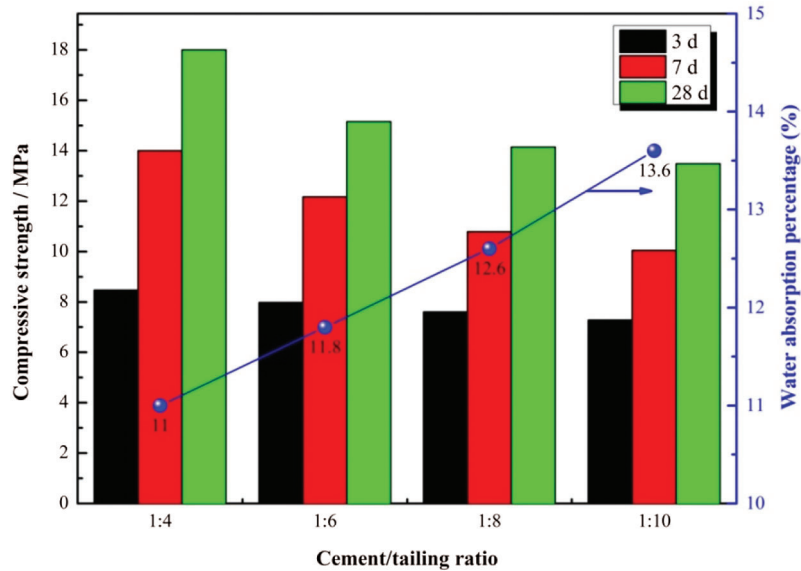


Figure 6: Effect of cement/tailing ratio on the UCS development and water absorption percentage of the baking-free bricks

Table 3: 3 days and 7 days UCS development rate of the baking-free brick specimens

Cement/tailing ratio	3 days strength development rate/%	7 days strength development rate/%
1:4	47.1	77.8
1:6	52.7	80.3
1:8	53.7	76.2
1:10	54.0	74.5

The 28 days UCS value (15.15 MPa) of the brick with the 1:6 cement/tailing ratio and 10% mixing water consumption is higher than those of the bricks using ordinary Portland cement, lime (natural hydraulic lime and calcareous lime), fly ash(or coal ash waste), and nano-SiO₂ as cementitious binders with similar fabrication parameters [13–19] although the size effect cannot be ignored. In general, different sample sizes cannot compare the strength values directly. According to the expressions converting the strength of cores into the strength of equivalent cubes in BS 1881:1983, the strength of cylinder is equal to 0.8 of the strength of a cube [30]. Also, the values of the cylinder and cube strength ratio are all about 0.8 in a table of equivalence of strengths of the two types of compression samples from the European standard BS EN 206-1:2000 [30]. Therefore, the mixed binder used in our experiments is an ideal material to stabilize gold mine tailings for the production of baking-free bricks.

In the entire cement/tailing ratio, the water absorption percentage increases continuously when the cement/tailings ratio decreases, as observed from Fig. 6. The highest water absorption percentage is reported around 13.6% at the cement/tailing ratio of 1:10. This result can be explained by Lang's study [19], revealing that the density of the cementing bricks is increased due to the introduction of a greater

amount of cementitious materials, and the micro- and macro cavities in the samples are reduced correspondingly. Less than 20% water absorption percentage is required in the Chinese standard GB/T 5101-2003 about the sintered common bricks. Therefore, all the water absorption percentages exhibited in the BC series samples meet the requirements of this standard completely. In general, low water absorption percentage of bricks implies a good ability to resist water infiltration.

3.3 Effect of Freezing-Thawing Cycle on the UCS of the Baking-Free Brick Specimens

Freezing-thawing resistance is another important performance of baking-free bricks. Freezing-thawing usually causes the damage of construction materials in many areas, especially in cold regions. Generally, the quality loss or the strength loss after the freezing-thawing cycle is used to characterize the freezing-thawing resistance of bricks. Figs. 7a, 7b illustrate the effect of freezing-thawing cycle and cement/tailing ratio on the UCS of the baking-free brick specimens under the dry-freezing condition, respectively. The BC series samples with a 1:6 cement/tailings ratio were used in the experiment of freezing-thawing cycle. As shown in Fig. 7a a progressive decrease in the UCS is observed as the freezing-thawing cycle increases. However, the magnitude of decrease is significantly different with the change of the freezing-thawing cycle. As the cycle time increase from 0 to 7 times, a slow decline from 15.15 MPa to 14.78 MPa generates. However, when the cycle time increases to 15 times, the UCS decreases to 13.80 MPa greatly and subsequently maintains a stable value at 20 cycles. Moreover, during the dry-freezing cycles, all the samples do not display remarkable damage on their surfaces. When the ambient temperature is below the freezing-point of the water in capillary pores, the volume expansion caused by a phase transition generates, producing expansion stress into the brick samples. Once the expansion stress is greater than the bond strength of the brick samples, small irreversible cracks will be generated around the capillary pores. When the ambient temperature exceeds the freezing-point, more water will migrate and fill into these capillary pores. It is expected that the UCS will decrease with the increasing freezing-thawing cycle inevitably.

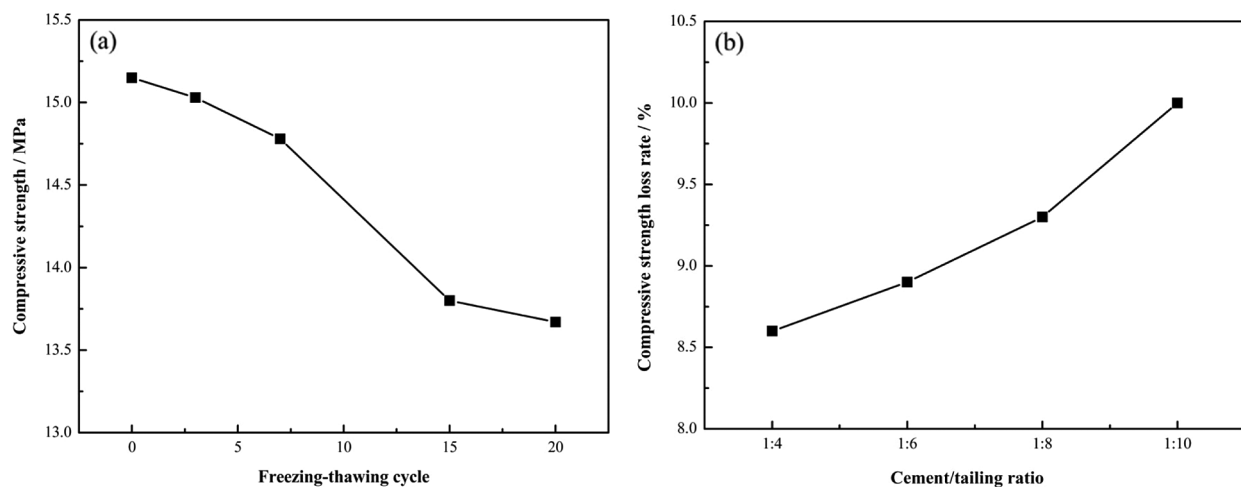


Figure 7: Effects of freezing-thawing cycle (a) and cement/tailing ratio (b) on the UCS (loss) of the baking-free brick specimens under the dry-freezing condition

It can be seen from Fig. 7b that the UCS loss rate gradually increases with the decrease of the cement/tailing ratio from 1:4 to 1:10. However, these data indicate that the damage of 20 freezing-thawing cycles for the baking-free bricks is in an acceptable range according to the Chinese standard JC/T 945-2005 (The strength loss rate of concrete solid bricks after 20 freeze-thaw cycles should $\leq 15\%$ for cold regions).

Therefore, the baking-free bricks prepared in our current work exhibit a good freezing resistance under the dry-freezing condition.

Figs. 8a, 8b illustrate the effect of freezing-thawing cycle and cement/tailing ratio on the UCS of the baking-free brick specimens under the wet-freezing condition, respectively. For the same test brick samples, the relationship between the freezing-thawing cycle time and the UCS under the wet-freezing condition is very similar to that under dry-freezing conditions, as shown in Figs.7a and 8a. However, the wet-frozen brick samples exhibit a lower strength compared with the dry-frozen brick samples, revealing that high water moisture content results in the deterioration in the UCS.

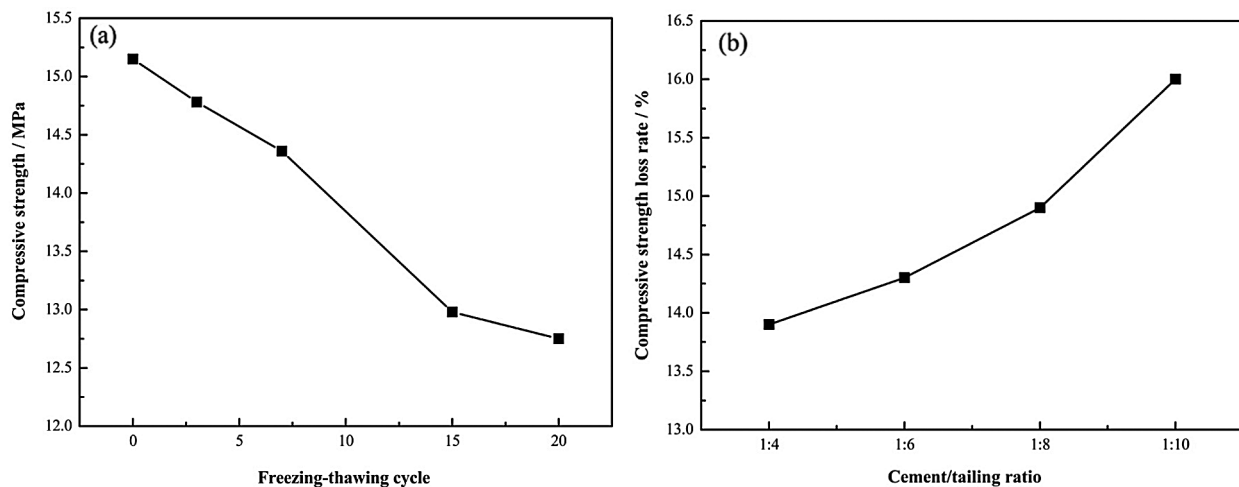


Figure 8: Effects of freezing-thawing cycle (a) and cement/tailing ratio (b) on the compressive strength (loss) of the baking-free brick specimens under the wet-freezing condition

Higher UCS loss rate under the wet-freezing condition can be seen by comparing Figs. 7b and 8b. Nevertheless, when reducing the cement/tailing ratio to 1:10, the UCS loss ratio cannot meet the requirements of the Chinese standard JC/T 945-2005. Too low a cement/tailing ratio will worsen the freezing resistance of the baking-free bricks.

In addition, steady increases in the UCS loss of around 8.6%–10.0% and 13.9%–16.0% when the brick samples undergo respectively 20 freezing-thawing cycles under the dry-freezing condition and the wet-freezing condition, which agree well with the tendency of water absorption percentage. Clearly, the higher the water absorption percentage of the brick samples, the higher the loss rate of freezing-thawing strength. This consistency can be explained based on the microstructure level. A higher water absorption percentage indicates that the brick samples have a looser microstructure and more interstices and hence the water will migrate to these interstices. When the water located in these interstices is frozen, local stress will be produced, leading to damage into the structure of the bricks.

3.4 Effect of Drying-Wetting Cycle on the UCS of the Baking-Free Brick Specimens

Drying-wetting resistance is also an important property of baking-free bricks. In the shallow ground, cyclic drying-wetting is a quite common phenomenon because of an alternation of dry and wet seasons. In this work, the drying-wetting cycles that the brick samples were subjected to were 0, 3, 5, 7, and 10 cycles. The variation in the UCS of the brick specimens with a 1:6 cement/tailing ratio after different drying-wetting cycles is shown in Fig. 9. With an increase in the drying-wetting cycles, the UCS of the brick specimens decreases exponentially. After 10 drying-wetting cycles, the UCS is about 13.48 MPa,

showing a low UCS loss rate of approximately 11%. The decrease in the UCS is related to the microstructural change of the brick samples. During the wetting process, the inclusion of the outside water damages the dense structure due to the overflow of the inside gas in the brick samples, causing the generation of pores. As a result, the cementitious materials existed the inside of the gold mine tailings will be overflowed owing to the inclusion of the water and the floating of the air [31]. However, it is observed that the decreasing degree of the UCS is gradually reduced after 7 drying-wetting cycles. The reason is that the microstructure of the brick sample is essentially stable after several drying-wetting cycles.

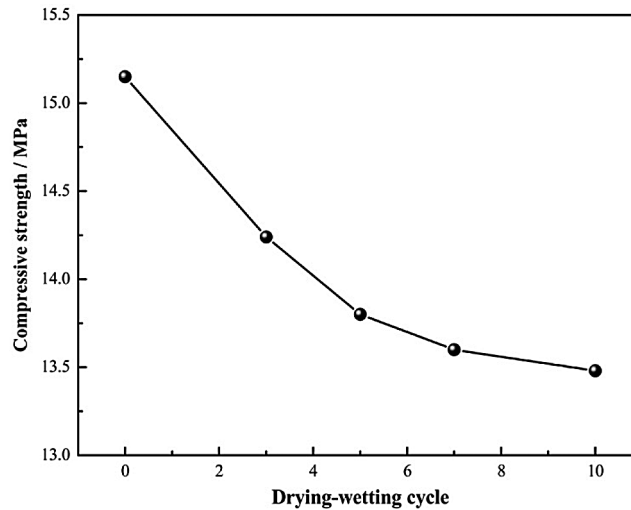


Figure 9: Variation in the compressive strengths of the brick specimens with the 1:6 cement/tailing ratio after different drying-wetting cycles

Fig. 10 shows the UCS of the brick samples subjected to 0 and 10 drying-wetting cycles. As seen in this figure, the UCS declines significantly with a decrease in the cement/tailing ratio whether the samples are subjected to any drying-wetting cycle or not. These variations corroborate the relationship between the UCS and the cement/tailing ratio. It is concluded that the cement/tailing ratio plays a significant role in the drying-wetting resistance of the baking-free bricks.

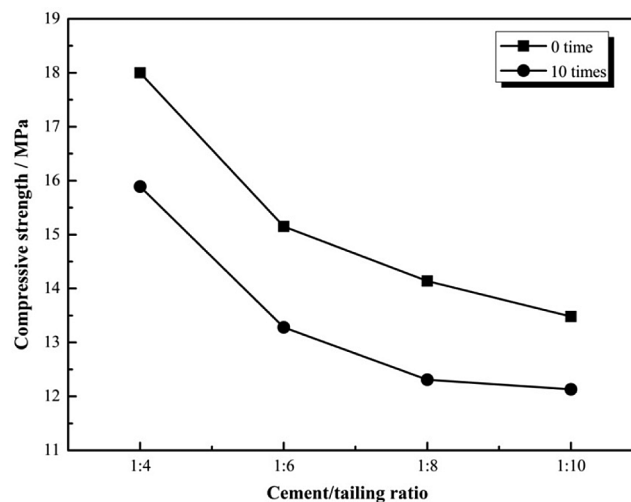


Figure 10: Compressive strengths of the brick samples subjected to 0 and 10 drying-wetting cycles

3.5 X-Ray Diffraction and Microstructure Analyses

To better understanding of the hydration reaction products of the baking-free bricks, X-ray diffraction (XRD) patterns analyses were conducted. The analyzed results of the phase composition for the BC series samples with the curing age of 28 days is presented in Fig. 11. The major minerals in the brick samples are quartz (SiO_2), which reveals the natural mineral composition of the gold mine tailings used in this work. Furthermore, some hydration products including CH, AFt, C-S-H, and C-A-S-H gels can be also distinguished in the brick samples, generating the internal driving force to ensure the strength development. With the increase of the cement/tailing ratio, the amount of C-S-H, C-A-S-H, and AFt increases. The hydration of the binders with low alkalinity used should be responsible for this observation. Initially, the clinker in the binders hydrates to generate CH[$\text{Ca}(\text{OH})_2$]. Then the quartz in the gold mine tailings dissolved in the liquid phase will combine with the generated CH to produce various types of CSH gels. Meanwhile, the pozzolanic activity of the quartz and Al_2O_3 in the composition is activated, and the secondary hydration reaction is generated by consuming CH. As a result, the amounts of C-S-H gels and C-A-S-H gels increase. Also, the C_3A in the clinker can react with gypsum, and water to generate ettringite (AFt) by the chemical activation of activators in the binders. Meanwhile, these findings can support the following leaching test results in this study. Additionally, the sanidine phase that existed in the gold mine tailings remains in the brick samples, indicating that it is an inert substance and does not participate in a hydration reaction.

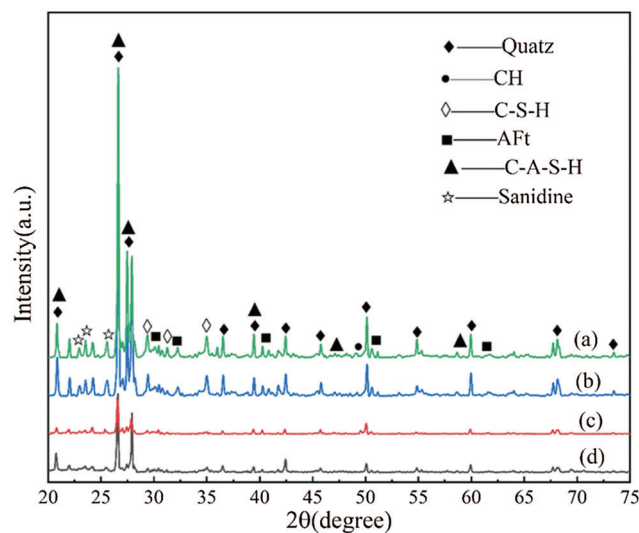


Figure 11: XRD patterns of the BC series samples with the curing age of 28 days: (a) 1:4; (b) 1:6; (c) 1:8; (d) 1:10

The fracture surface morphologies of the BC series samples after 3 days and 28 days of curing age were observed using SEM technology and the results are shown in Figs. 12–15. It is seen that loose structures with a few pores can be found when the brick samples are cured for 3 days. When the curing age rises to 28 days, dense structures with few pores are observed except the sample with the cement/tailings ratio of 1:10. Oti et al. [32] revealed that the phenomena presented in the XRD results would promote a denser microstructure with fewer pores and voids. They pointed out that the stronger bonds were formed and the possibility of pozzolanic C-S-H during the hydration process was improved, and therefore good mechanical and durability could be obtained for the baking-free bricks. Our investigation in this work on the strength development, water absorption, freezing-thawing resistance, and drying-wetting resistance is highly consistent with their findings.

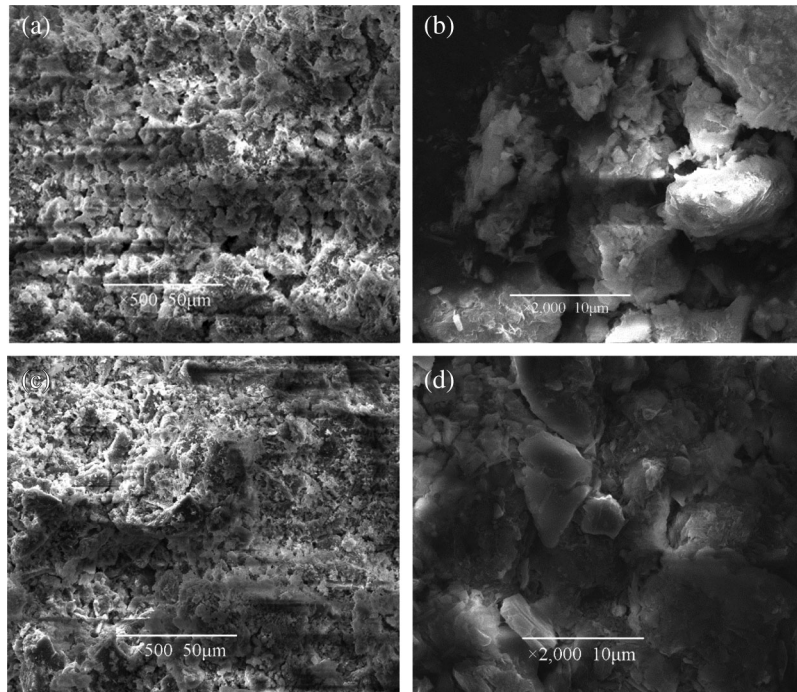


Figure 12: SEM images of the BC series samples with the cement/tailing ratio of 1:4 after 3 days [(a) and (b)] and 28 days [(c) and (d)] curing ages

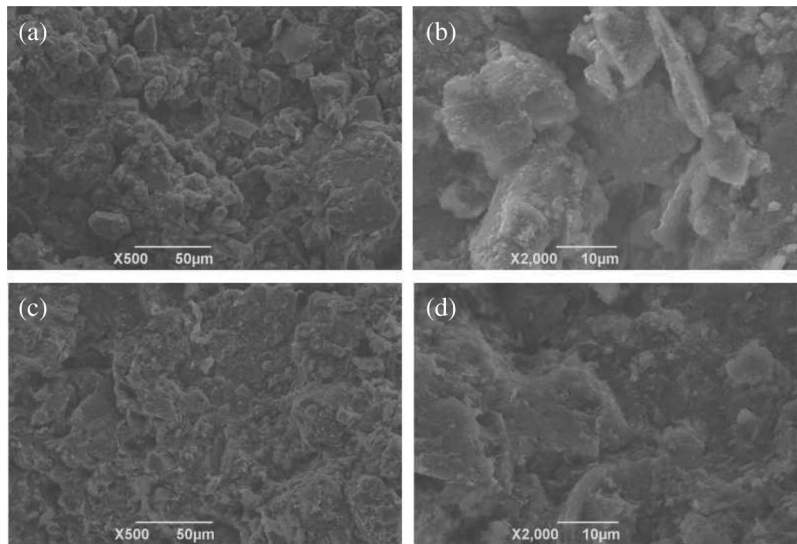


Figure 13: SEM images of the BC series samples with the cement/tailing ratio of 1:6 after 3 days [(a) and (b)] and 28 days [(c) and (d)] curing ages

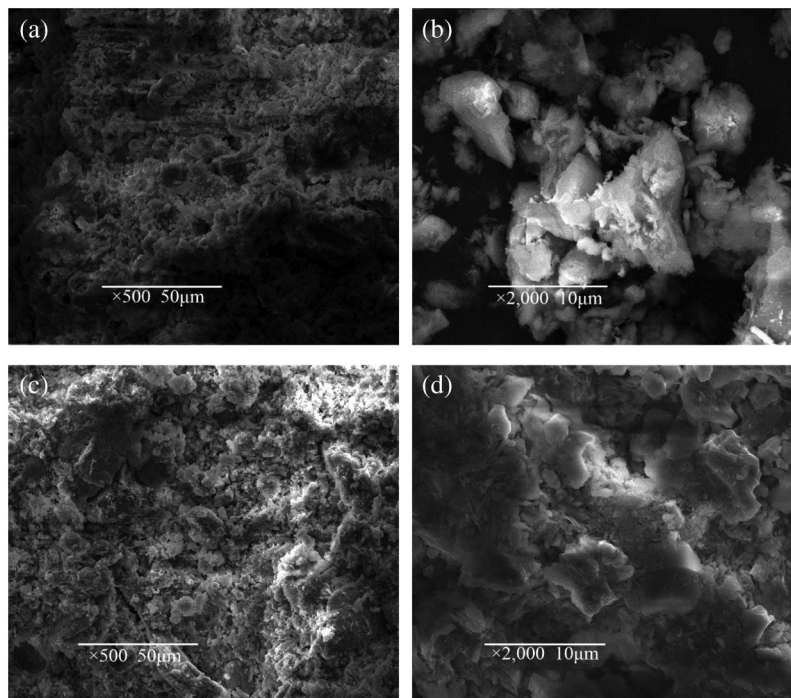


Figure 14: SEM images of the BC series samples with the cement/tailing ratio of 1:8 after 3 days [(a) and (b)] and 28 days [(c) and (d)] curing ages

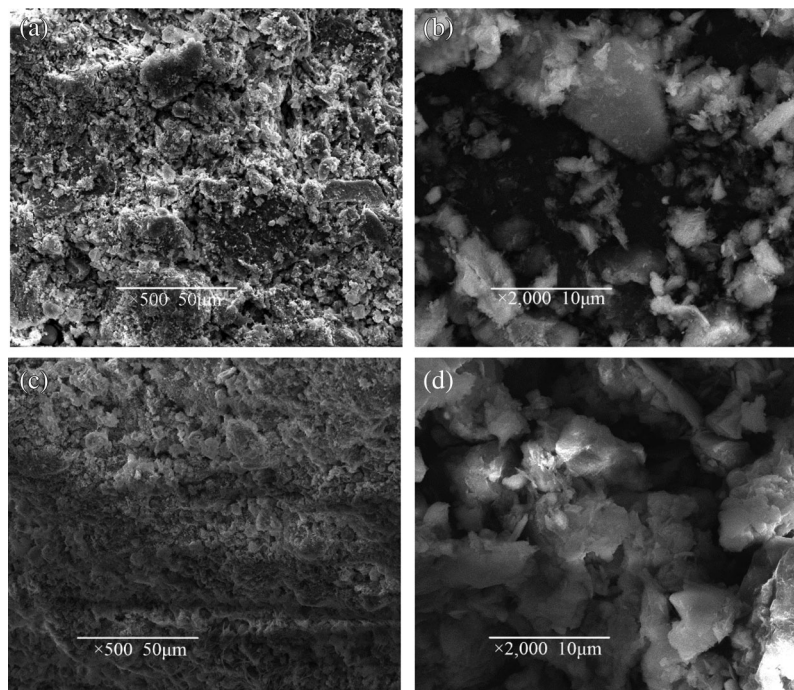


Figure 15: SEM images of the BC series samples with the cement/tailing ratio of 1:10 after 3 days [(a) and (b)] and 28 days [(c) and (d)] curing ages

3.6 Potential Environmental Effect of Baking-Free Bricks

The baking-free brick sample with a cement/tailings ratio of 1:6 and a mixing water consumption of 10% cured for 28 days, which is the mix design that yielded the favorable comprehensive properties, was evaluated for environmental effect. The concentrations of leached heavy metals in the leachate of the baking-free brick sample are presented in Table 4. As can be seen, the test results show the low concentrations of heavy metals, which are below the Chinese standard GB 5085.3-2007 allowable concentrations in the leachate. These test results also indicate that the baking-free bricks prepared by the gold mine tailings and the cemented materials with low alkalinity are stable for release risk of hazardous metals and will not leach to the environment.

Table 4: Leaching concentrations of the baking-free bricks

	Baking-free bricks	GB 5085.3-2007 maximum allowed concentration in leachate (mg/L)
As	0.71	5
Cr	0.07	5
Cu	0.02	100
Zn	0.02	100
Pb	ND	5
Ba	0.04	100
Cd	ND	5
Mn	0.18	5

4 Conclusions

This investigation successfully fabricated the baking-free bricks made from gold mine tailings and slag powder-cement-fly ash binders along with a small amount of chemical activators. A series of experimental tests were carried out to study the influences of mixing water consumption, and the cement/tailing ratio on the water absorption percentage, unconfined compressive strength, freezing-thawing resistance, and drying-wetting resistance of the baking-free bricks. Furthermore, the phase composition and microstructure of the typical baking-free brick samples were also evaluated using X-ray diffraction (XRD) and scanning electron microscopy (SEM) techniques. The main conclusions in this investigation were summarized as follows:

1. A binder with slag powder and fly ash wastes blended with cement and chemical additives showed an ability to stabilize gold mine tailings. Therefore, our study provided a technical strategy for the efficiently comprehensive utilization of industrial waste and mine waste.
2. Mixing water consumption is one of the significant factors to influence the performances of the baking-free bricks. The 28 days unconfined compressive strength of the baking-free bricks increased from 13.17 MPa to 15.15 MPa as the mixing water consumption increased from 6% to 10%. However, the unconfined compressive strength sharply decreased from 15.15 MPa to 12.22 MPa as the mixing water consumption was 12%.
3. The unconfined compressive strength decreased with the decrease of the cement/tailing ratio. However, the effect of the cement/tailings ratio on the strength development of the brick sample

with various curing ages was different. Compared with the cement/tailing ratio, the curing age had a more significant effect on the early strength of the baking-free bricks.

4. The unconfined compressive strength of the baking-free brick specimens decreased with the increase of times of freezing-thawing cycle or drying-wetting cycle. The damage of 20 freezing-thawing cycles or 10 drying-wetting cycles for the baking-free bricks was in an acceptable range ($\leq 15\%$ strength loss rate), exhibiting good freezing-thawing and drying-wetting resistances.

Funding Statement: This work was financial supported by the Key Research and Development Program of Anhui Province (No. 202004a07020039).

Conflicts of Interest: The authors declare that they have no conflicts of interest to report regarding the present study.

References

1. Wei, Z. A., Zhao, J. K., Wang, W. S., Yang, Y. H., Zhuang, S. N. et al. (2021). Utilizing gold mine tailings to produce sintered bricks. *Construction and Building Materials*, 282(4), 122655. DOI 10.1016/j.conbuildmat.2021.122655.
2. Lu, Y., Li, G., Liu, W., Yuan, H. Y., Xiao, D. (2018). The application of microwave digestion indecomposing some refractory ore samples with solid fusion agent. *Talanta*, 186, 538–544. DOI 10.1016/j.talanta.2018.03.074.
3. Deng, K., Yin, P., Liu, X. G., Tang, Q. H., Qu, R. J. (2014). Modeling, analysis and optimization of adsorption parameters of Au(III) using low-cost agricultural residuals buckwheat hulls. *Journal of Industrial Engineering Chemistry*, 20(4), 2428–2438. DOI 10.1016/j.jiec.2013.10.023.
4. Zheng, W. X. (2013). Analysis of the proportion of aerated concrete block materials produced by using gold tailings. *Science & Technology Vision*, 8(9), 18–19 (in Chinese). DOI 10.19694/j.cnki.issn2095-2457.2013.08.009.
5. Guo, X. Y., Qin, H., Tian, Q. H., Zhang, L. (2020). The efficacy of a new iodination roasting technology to recover gold and silver from refractory gold tailing. *Journal of Cleaner Production*, 261(2), 121147. DOI 10.1016/j.jclepro.2020.121147.
6. Yang, F. H., Liang, X. Y., Zhu, Y., Wang, C. L., Zhao, G. F. et al. (2019). Preparation of environmentally friendly and energy-saving autoclaved aerated concrete using gold tailings. *Journal of New Materials for Electrochemical Systems*, 22(3), 159–164. DOI 10.14447/jnmes.v22i3.a08.
7. Gitari, M. W., Akinyemi, S. A., Thobakgale, R., Ngoejana, P. C., Ramugondo, L. et al. (2018). Physicochemical and mineralogical characterization of Musina minecopper and New Union gold mine tailings: Implications for fabrication of beneficial geopolymeric construction materials. *Journal of African Earth Sciences*, 137(3), 218–228. DOI 10.1016/j.jafrearsci.2017.10.016.
8. Çelik, Ö., Elbeyli, I. Y., Piskin, S. (2006). Utilization of gold tailings as an additive in Portland cement. *Waste Management Research*, 24(3), 215–224. DOI 10.1177/0734242X06064358.
9. Shao, H., Liang, K., Peng, F., Zhou, F., Hu, A. (2005). Production and properties of cordierite-based glass-ceramics from gold tailings. *Minerals Engineering*, 18(6), 635–637. DOI 10.1016/j.mineng.2004.09.007.
10. Kim, Y., Kim, M., Sohn, J., Park, H. (2018). Applicability of gold tailings, waste limestone, red mud, and ferronickel slag for producing glass fibers. *Journal of Cleaner Production*, 203(30), 957–965. DOI 10.1016/j.jclepro.2018.08.230.
11. Oti, J. E., Kinuthia, J. M., Bai, J. (2008). Using slag for unfired-clay masonry-bricks. *Construction and Building Materials*, 161(4), 147–155. DOI 10.1680/coma.2008.161.4.147.
12. Pimraksa, K., Chindaprasirt, P. (2009). Lightweight bricks made of diatomaceous earth, lime and gypsum. *Ceramics International*, 35(1), 471–478. DOI 10.1016/j.ceramint.2008.01.013.
13. Miqueleiz, L., Ramirez, F., Oti, J. E., Seco, A., Kinuthia, J. M. et al. (2013). Alumina filler waste as clay replacement material for unfired brick production. *Engineering Geology*, 163(6), 68–74. DOI 10.1016/j.enggeo.2013.05.006.
14. Wang, W. J., Gan, Y. X., Kang, X. (2021). Synthesis and characterization of sustainable eco-friendly unburned bricks from slate tailings. *Journal of Materials Research and Technology*, 14(2), 1697–1708. DOI 10.1016/j.jmrt.2021.07.071.

15. Wattanasiriwech, D., Saiton, A., Wattanasiriwech, S. (2009). Paving blocks from ceramic tile production waste. *Journal of Cleaner Production*, 17(18), 1663–1668. DOI 10.1016/j.jclepro.2009.08.008.
16. Kang, X., Gan, Y. X., Chen, R. P., Zhang, C. (2021). Sustainable eco-friendly bricks from slate tailings through geopolymerization: Synthesis and characterization analysis. *Construction and Building Materials*, 278(4), 122337. DOI 10.1016/j.conbuildmat.2021.122337.
17. Raut, S. P., Sedmake, R., Dhunde, S., Ralegaonkar, R. V., Mandavgane, S. A. (2012). Reuse of recycle paper mill waste in energy absorbing light weight bricks. *Construction and Building Materials*, 27(1), 247–251. DOI 10.1016/j.conbuildmat.2011.07.053.
18. Zhou, J., Gao, H., Shu, Z., Wang, Y., Yan, C. (2012). Utilization of waste phosphogypsum to prepare non-fired bricks by a novel hydration-recrystallization process. *Construction and Building Materials*, 34(6), 114–119. DOI 10.1016/j.conbuildmat.2012.02.045.
19. Lang, L., Chen, B., Pan, Y. J. (2020). Engineering properties evaluation of unfired sludge bricks solidified by cement-fly ash-lime admixed nano-SiO₂ under compaction forming technology. *Construction and Building Materials*, 259(1), 119879. DOI 10.1016/j.conbuildmat.2020.119879.
20. Guo, L., Chen, P. P., Guo, L. X., Xue, Z. L., Guan, Z. et al. (2021). Pore structure characteristics of baking-free slag-sludge bricks and its correlations to mechanical properties. *Journal of Renewable Materials*, 9(10), 1805–1819. DOI 10.32604/jrm.2021.015140.
21. Maierdan, Y., Haque, M. A., Chen, B., Maimaitiyiming, M., Ahmad, M. R. (2020). Recycling of waste river sludge into unfired green bricks stabilized by a combination of phosphogypsum, slag, and cement. *Construction and Building Materials*, 260, 120666. DOI 10.1016/j.conbuildmat.2020.120666.
22. Peng, Y. Z., Peng, X., Yang, M., Shi, H. L., Wang, W. C. et al. (2020). The performances of the baking-free bricks of non-sintered wrap-shell lightweight aggregates from dredged sediments. *Construction and Building Materials*, 238(4), 117587. DOI 10.1016/j.conbuildmat.2019.117587.
23. Ashour, T., Korjenic, A., Korjenic, S., Wu, W. (2015). Thermal conductivity of unfired earth bricks reinforced by agricultural wastes with cement and gypsum. *Energy and Buildings*, 104(5), 139–146. DOI 10.1016/j.enbuild.2015.07.016.
24. Zhao, H., Gou, H. Y. (2021). Unfired bricks prepared with red mud and calcium sulfoaluminate cement: Properties and environmental impact. *Journal of Building Engineering*, 38(7), 102238. DOI 10.1016/j.jobbe.2021.102238.
25. Liu, Z. H., Chen, Q. Y., Xie, X. B., Xue, G., Du, F. F. et al. (2011). Utilization of the sludge derived from dyestuff-making wastewater coagulation for unfired bricks. *Construction and Building Materials*, 25(4), 1699–1706. DOI 10.1016/j.conbuildmat.2010.10.012.
26. Debasis, D., Sreenivas, S., Gautam, K. D., Sandeep, P. (2017). Paste backfill technology: essential characteristics and assessment of its application for mill rejects of uranium ores. *Transactions of the Indian Institute Metals*, 70(2), 487–495. DOI 10.1007/s12666-016-0999-0.
27. Zhang, Z., Qian, J., You, C., Hu, C. (2012). Use of circulating fluidized bed combustion fly ash and slag in autoclaved brick. *Construction and Building Materials*, 35(7), 109–116. DOI 10.1016/j.conbuildmat.2012.03.006.
28. Zhao, F., Zhao, J., Liu, H. (2009). Autoclaved brick from low-silicon tailings. *Construction and Building Materials*, 23(1), 538–541. DOI 10.1016/j.conbuildmat.2007.10.013.
29. Kim, S. Y., Jun, Y., Jeon, D., Oh, J. E. (2017). Synthesis of structural binder for red brick production based on red mud and fly ash activated using Ca(OH)₂ and Na₂CO₃. *Construction and Building Materials*, 147(11), 101–116. DOI 10.1016/j.conbuildmat.2017.04.171.
30. Neville, A. M. (2012). *Properties of concrete (5th Edition)*. England: Longman Press.
31. Tang, Y. C., Zhang, Z. J., An, P. E., Dou, M. Q., Zhou, H. (2018). Experimental research on strength characteristics of tailings sand under the effect of wetting and drying cycles. *Journal of University of South China (Science and Technology)*, 32, 10–14 (in Chinese). DOI 10.19431/j.cnki.1673-0062.2018.01.002.
32. Oti, J. E., Kinuthia, J. M., Bai, J. (2009). Compressive strength and microstructural analysis of unfired clay masonry bricks. *Engineering Geology*, 109(3–4), 230–240. DOI 10.1016/j.enggeo.2009.08.010.